The 11th Canadian Conference on Earthquake Engineering

Canadian Association for Earthquake Engineering

INFLUENCE OF AXIAL COMPRESSIVE STRESS ON THE IN-PLANE SHEAR PERFORMANCE OF REINFORCED MASONRY SHEAR WALLS

Hany M. Seif ElDin
PhD Candidate, Concordia University, Canada
h_seif@encs.concordia.ca

Khaled Galal
Professor, Concordia University, Canada
galal@bcee.concordia.ca

ABSTRACT: Similar to reinforced concrete (RC) buildings, shear walls are a popular lateral load resisting system for reinforced masonry (RM) structures. There are several failure modes for RM shear walls. One of the possible failure mechanisms is the diagonal shear failure. The shear behaviour of RM shear walls at the plastic hinge zone is more complicated than RC shear walls due the interaction between the nonlinear responses of their constituent materials, namely; concrete masonry blocks, mortar, grout, and steel reinforcement. This paper is part of a research program investigating the shear behaviour of fully grouted RM shear walls subjected to the combined effects of axial load and in-plane cyclic lateral excitations. Three full-scale fully grouted rectangular RM shear walls were tested under axial compressive stress of 0.0, 1.0, and 1.5 MPa, respectively. The test results of the three tested RM walls are presented and discussed to evaluate the influence of the axial compressive stress on the in-plane shear performance of RM shear walls.
Keywords: Reinforced Masonry; Shear walls; Compressive stress; and Shear performance.

1. Introduction

Similar to reinforced concrete (RC) buildings, shear walls are key structural elements that are commonly used in RM buildings to resist the lateral loads. Over the past decades, many research works have been conducted to investigate the seismic performance of the RM shear walls to enhance their lateral strength, stiffness, and energy dissipation (Mayes et al., 1976; Priestley and Elder, 1982; Shing et al. 1989; and El-Dakhakhni et al. 2013). The results of the conducted research programs have led to a marked increase in the number of multi-story RM buildings that are capable of resisting higher seismic loads. The flexural behaviour of RM shear walls with high shear span-to-depth ratio is well defined and follows the simple flexural theory of RC structures based on the plane-section assumptions. On the other hand, the shear behaviour of RM shear walls exhibits a more brittle and complex behaviour. Seif ElDin and Galal (2015) conducted a survey of the design equations provided in design standards and proposed by researchers for the in-plane shear capacity of RM shear walls. Their study highlighted the parameters that influence the shear behaviour of RM shear walls, i.e. the level of the axial compressive stress, the grouting pattern, the shear span to depth ratio, the amount of transverse and vertical reinforcement, and the wall aspect ratio.

Most of the available equations for the in-plane shear strength of masonry, V_m, including the Canadian Standard CSA S304-14 and the Masonry Standards Joint Committee MSJC-2013, take into account the favourable influence of the axial compressive stress, σ_n, on the shear strength. An independent component of 25% of σ_n is considered to contribute to the shear capacity. Fig. 1 shows the principal stresses acting on a masonry panel where a two-dimensional state of stress develops in the wall: axial compressive stress, σ_n, and shear stress, v.
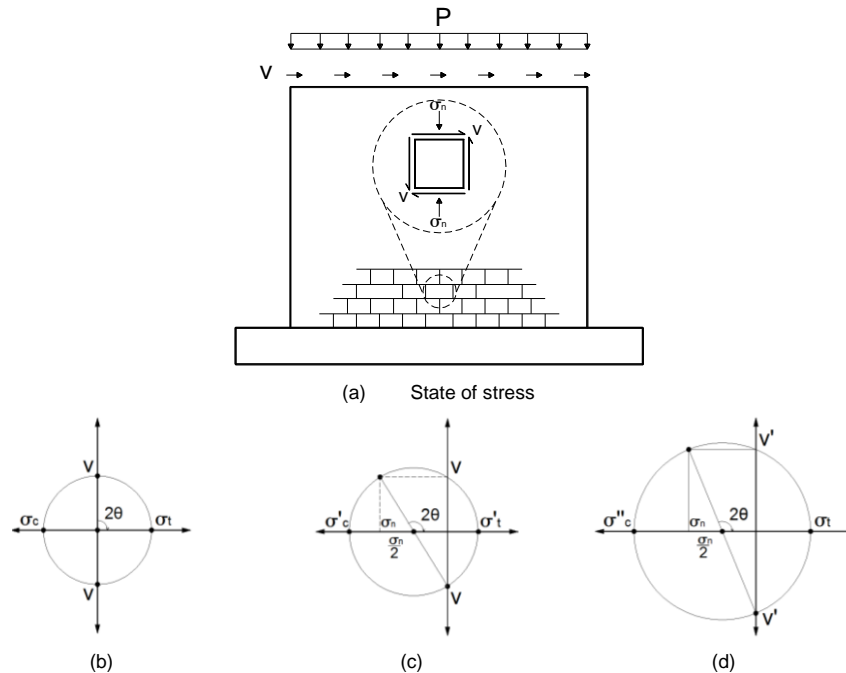
Fig. 1 –Principal stresses acting on the masonry wall

When the principal tensile stress, σ_t, exceeds the tensile strength of masonry, the initiation of diagonal shear cracks takes place in masonry walls. As shown in Fig.1-c, the presence of the axial compressive load, P, increases the principal compressive stresses to be σ'_c, while it reduces the principal tensile stresses to be σ'_t due the compressive field created by the axial compression load. Consequently, to reach the same tensile strength, a higher value of lateral load is required, v' (see Fig. 1-d). In addition, increasing the level of the axial compressive stress increases the angle of the principal stresses, θ. Many research works have been carried out to quantify the contribution of the axial compressive stresses toward better estimating the shear capacity of RM shear walls (Banting and El-Dakhakhni 2013).

Matsumura (1988) tested 80 masonry walls to evaluate their seismic performance under in-plane loads. Out of the 80 walls, 14 fully grouted concrete masonry walls failed in shear. One of the studied parameters was the influence of the compressive axial stress. The axial stress ranged from 0.49 to 1.96 MPa. Based on regression analysis of the test results, Matsumura (1988) assumed that 20% of the axial compression load contributes toward the shear strength of the masonry walls. Shing et al. (1990) carried out in-plane cyclic lateral loading on 22 RM walls to investigate the inelastic flexural and shear behaviour of concrete masonry shear walls. All the walls were fully grouted with uniform distributed vertical and lateral reinforcement. The axial stresses on the tested masonry walls varied from 0.0 to 1.93 MPa. Unlike Matsumura (1988), Shing et al. (1990) did not consider a separate component for the axial compressive stress. Instead, it was included in the masonry contribution. Anderson and Priestly (1992) used the experimental test results of Sveinssion et al. (1985), Matsumura (1987), and Shing et al. (1990) to develop an equation for calculating the shear strength of the RM shear walls under in-plane lateral loads. This equation is widely used in North America Masonry Standards with slight modification. A higher contribution of the axial compression load, 25%, was proposed by Anderson and Priestly (1992) compared to 20% that was previously proposed by Matsumura (1988). Using the test results of eight fully grouted and two partially grouted full-scale RM walls, Voon and Ingham (2007) proposed a design expression for the in-plane shear strength of RM walls. Three values of the axial compressive stress 0.0, 0.25, and 0.5 MPa were considered in their study. Unlike most of the existing design equations for the in-plane shear strength, the proposed contribution of the axial compressive stress was considered to be dependent upon the angle that will be formed between the wall axis and the strut from the point of load application to the center of the flexural compression zone at the wall's plastic hinge critical section. This proposed contribution is based on a study conducted by Priestley et al. (1994) for the seismic shear strength of RC columns. This paper aims to investigate the influence of the axial compressive stress on

the in-plane shear performance of RM shear walls including its effect on the lateral stiffness, strength, crack propagation, displacement ductility, and the contribution of the transverse reinforcement to the shear capacity.

2. Experimental work

2.1. Test Layout

Throughout the experimental work, three full-scale fully grouted rectangular RM shear walls were tested to evaluate the influence of the axial compressive stress on the in-plane shear performance of RM shear walls. The RM walls were tested under axial compressive stress of 0.0, 1.0, and 1.5 MPa, respectively. All the tested walls had the same dimensions of 1.8m x 1.6m x 0.19m and were vertically reinforced with 20M bar in each cell with a flexural reinforcement ratio of 0.79% (as shown in Fig. 2).The walls have transverse reinforcing steel bar of 10M uniformly distributed at 400 mm c/c along the height of the wall. The transverse bars were hooked using the standard 180° hook around the outermost wall flexural reinforcing bars. Each of the tested walls was constructed on a rigid RC foundation that was designed to remain un-cracked during testing. Table 1 summarizes the test matrix including the walls dimensions, the reinforcement details, and the applied compression axial stress.
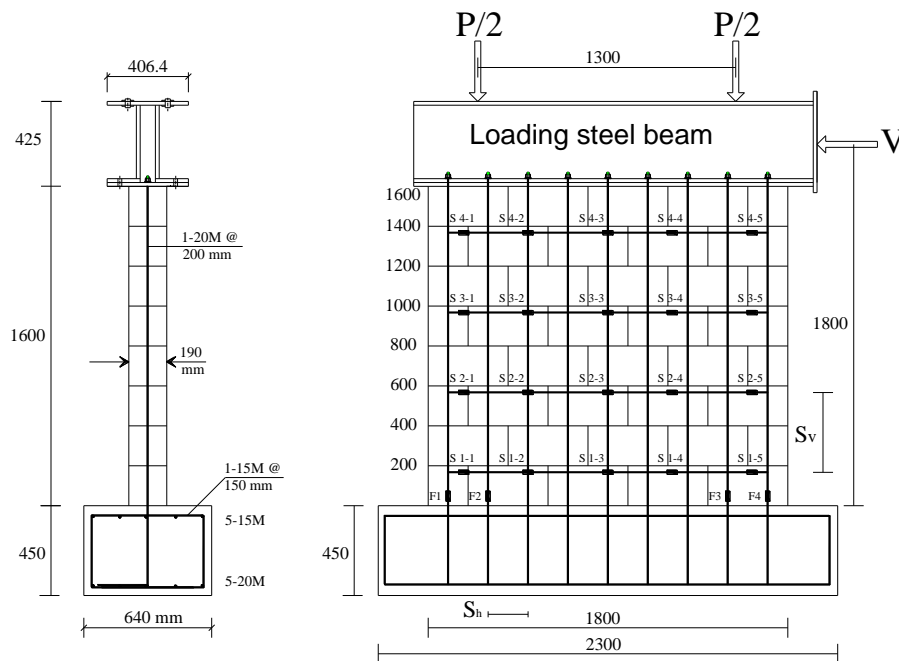
Fig. 2–Typical tested wall dimensions

Table 1- Test Matrix

Specimen	Wall dimensions			Reinforcement		Axial Stress
	H	L_w	Effective width	Vertical	Horizontal	σ_n
Units	mm	mm	mm	---	---	MPa
W- σ_n0	1600	1800	190	20M@200	10M@400	0.0
W-σ_n1.0	1600	1800	190	20M@200	10M@400	1.0
W-σ_n1.5	1600	1800	190	20M@200	10M@400	1.5

2.2. Material Properties

All the tested walls and the required auxiliary specimens were constructed using lightweight knock-out concrete masonry units (CMUs) with a nominal dimensions of 390mm × 190mm × 190mm. These Knock-out units are masonry units that have knock-out webs which can be removed to accommodate the transverse reinforcement (see Fig. 3). In addition, these types of units are providing grouting continuity in the vertical and horizontal directions, preventing any weakness planes between the concrete masonry units. The blocks were joined together with 10mm type S mortar joints and laid in a running bond pattern. Table 2 summarizes the properties of the constituent materials.
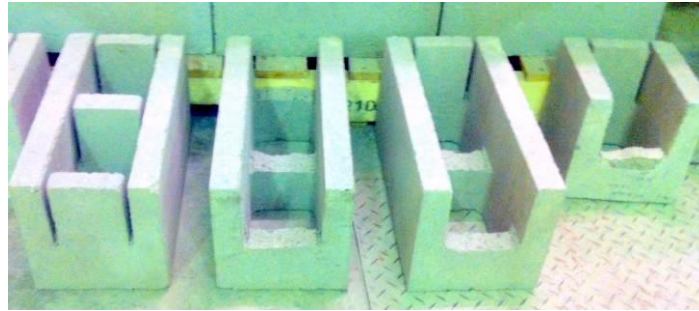
Fig. 3– Full-scale concrete masonry units (CMUs) with knock-out webs

Table 2- Properties of the constituent materials

Material	Strength (C.O.V)	Standard test
Type S Mortar	7d- 8.5 MPa (8.8%) 28d- 13.7 MPa (7.8%)	Cube Compressive Strength ASTM C780-09
	112.16% (3.8%)	Flow Table Test ASTM 1437-07
Knock out concrete block	12.9 kg (3.1%)	Weight
	16.7 MPa (4.8%)	Block Compressive Strength ASTM C140-10
Footing Concrete	7d- 30.5 MPa (5.1%) 28d- 39.5 MPa (6.6%)	Compressive strength
	28d- 4.2 MPa (4.4%)	Splitting tensile strength
coarse grout	7d- 21.6 MPa (8.4%) 28d- 29.4 MPa (7.3%)	Cylinder Compressive Strength ASTM C39-10
Steel Reinforcement	430 MPa (3.2%)	Yield strength ASTM A615-09
	196 GPa (1.85%)	Modulus of Elasticity ASTM A615-09
	536 MPa (2.7%)	Ultimate strength ASTM A615-09
4-Course Running Bond Prism	13.1 MPa (7.6%)	Prism Compressive strength , $f_m^{'}$, ASTM C1314-10
	0.0025 (11.4%)	Axial strain at maximum strength, ε_o
	6.93 GPa	Modulus of elasticity, E_m ,

2.3. Test Setup

Three MTS hydraulic actuators were used to apply the loads as shown Fig. 4. Two actuators were installed vertically and were used to apply the axial compression force on the top of the wall. A horizontal actuator was used to apply the cyclic horizontal excitations. All the loads were transferred to the tested walls through a built-up steel loading beam that was connected to the top of the wall. The three actuators were synchronized to apply the lateral cyclic forces while maintaining a constant axial load. To prevent

any out of plane displacement, two out of plane back-to-back steel angles were connecting the loading beam (through slotted holes) to a strong resistance concrete wall.

Two different types of instrumentations were used to monitor the deformations of the tested walls. Nine potentiometers were attached to each wall to measure the horizontal, vertical, and diagonal displacements. The applied lateral displacement was measured as the difference between the average reading of the top displacements from both directions of loading. Four strain gauges were installed at the wall-footing interface of the two outermost vertical reinforcement bars in each side, to define the yield displacement. For adequate monitoring of the axial strain distribution along the transverse reinforcement, five 5mm strain gauges were distributed equally along the total length of each bar. Using the experimentally measured stress-strain curve and cross-section area for the steel reinforcing bars, the transverse reinforcement contribution to the in-plane shear strength was calculated. The loads were applied in two phases. In the first phase, the total vertical compression load was applied using load-control protocol. Next, the test protocol was switched to displacement-control. In the second phase, in-plane lateral displacements were introduced at the middle height of the loading steel beam, according to the loading histories proposed by FEMA 461. In each stage of lateral loading, two displacement cycles were completed for each target displacement increment.
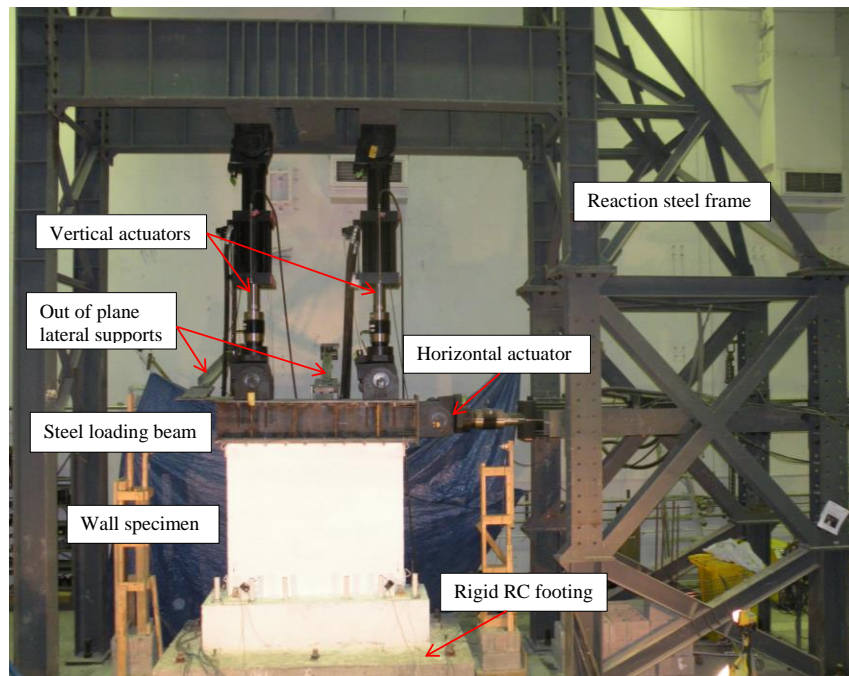
Fig. 4 –Test setup for the tested RM shear walls

3. Experimental Results

The experimentally recorded data for the displacement, lateral load resistance, and ductility are presented in Table 3. In addition, Fig. 5 shows the hysteresis lateral load-displacements loops along with the backbone envelopes for the tested walls. The three tested walls had typical hysteretic response with generally symmetrical hysteretic loops in the reversed directions of loading. Hence, the data for the push loading direction were selected to be presented in this paper to make it easier to follow and compare. The lateral yield displacement was taken as the average between the top lateral displacements for both the +ve and -ve cycles that are corresponding to the initial yield of tension vertical reinforcement. Failure was defined as the point on the loading curve where the lateral resistance dropped to 80% of the maximum lateral (peak) load recorded, in whichever direction this occurred first. All the measured displacements shown in Table 3 are normalized to the wall height.

Table 3- Summary of test results

Wall	Δ_y	Q_y	Q_u	Δ_{Qu}	$\Delta_{80\%Qu}$	$\mu_{\Delta Qu}$	$\mu_{\Delta 80\%Qu}$	$\mu_{\Delta 1\%}$
W- σ_n0	0.26	254	345	0.63	1.08	2.4	4.1	3.8
W-σ_n1.0	0.29	328	418	0.88	1.23	3.0	4.2	3.4
W-σ_n1.5	0.31	365	458	0.75	1.08	2.8	3.4	3.2
Units	%H	kN	kN	%H	%H	---	---	---

Δ_y,   lateral yield displacement, it was taken as the average between the top lateral displacements that are corresponding to the first yield in the vertical reinforcement in each direction,

Q_y,   lateral yield load, at the lateral yield displacement,

Q_u,   lateral peak load,

Δ_{Qu},   top lateral displacement at the peak lateral load, Q_u,

$\Delta_{80\%Qu}$,   top lateral displacement defined at a drop in wall capacity to 80% of Q_u,

$\mu_{\Delta Qu}$,   lateral displacements ductility at peak load,

$\mu_{\Delta 80\%Qu}$ lateral displacements ductility at a drop in wall capacity to 80% of Q_u, and

$\mu_{\Delta 1\%}$ lateral displacements ductility at a drift limit of 1.0%

(a)   Wall W-σ_n0

(b)   Wall W-σ_n1

(c)   Wall W-σ_n1.5
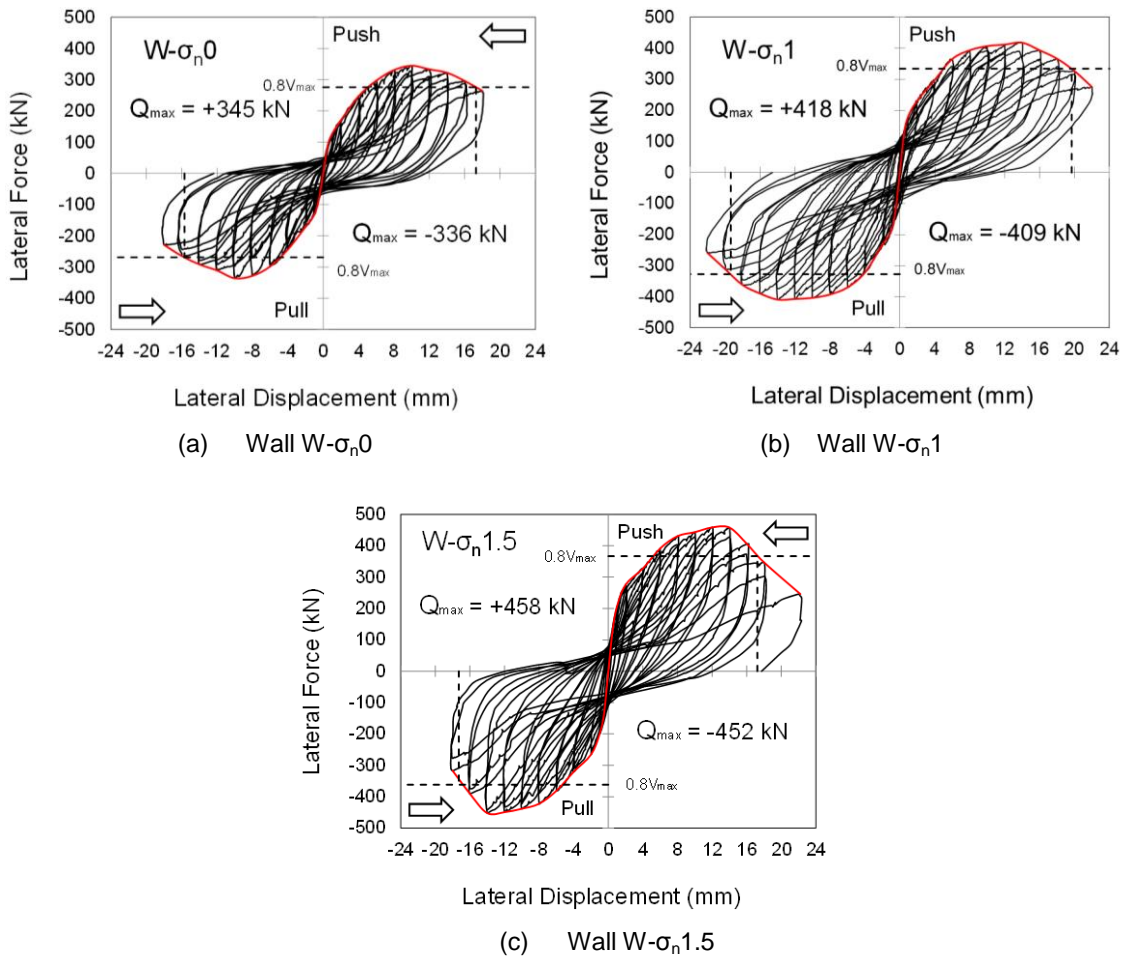
Fig. 5 – Lateral load-displacement hysteretic relationships and the backbone envelopes

As shown in Table 3 and Fig. 5, the axial compressive stress has a positive influence on the lateral load resistance. Increasing the axial compressive stress from 0.0 to 1.0 and 1.5 MPa, the maximum recorded lateral load resistance increased from 345 to 418 and 458 kN, respectively. Similar influence can be noticed on the yield capacity. The measured average yield displacement and the corresponding lateral load for wall W-σ_n0 were 4.2 mm and 254 kN, respectively. These values increased to 4.7 mm and 328 kN for wall W-σ_n1.0 and 5.0 mm and 365 kN for wall W-σ_n1.5. As expected, increasing the axial compression level has a negative effect on the lateral displacements ductility at a drift limit of 1.0% where it decreased from 3.8% to 3.4% and 3.2% for walls W-σ_n0, W-σ_n1.0, and W-σ_n1.5, respectively. Fig. 6 shows the cracking patterns at different stages; the first major diagonal crack, lateral peak load, and when the lateral load dropped to 80% of Q_u for the three tested walls.

W-σ_n0.0 Δ = +3.0 mm   W-σ_n1.0 Δ = +3.2 mm   W-σ_n1.5 Δ = +3.4 mm

(a)

W-σ_n0.0 Δ = +10.0 mm   W-σ_n1.0 Δ = +14.0   W-σ_n1.5 Δ = +14.0 mm

(b)

W-σ_n0.0 Δ = +17.3 mm   W-σ_n1.0 Δ = +19.7   W-σ_n1.5 Δ = +17.2 mm

(c)
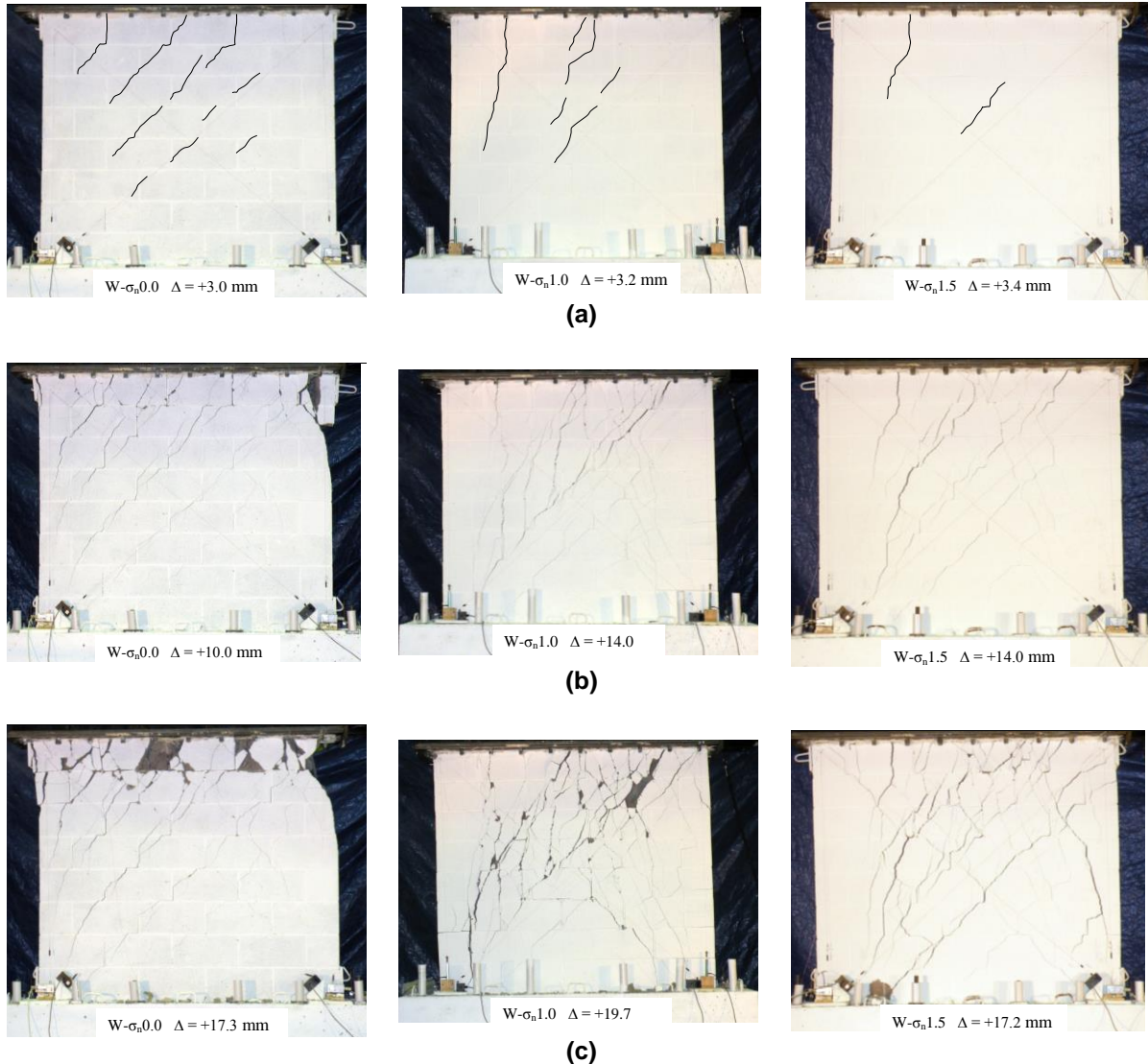
Fig. 6 – The cracking patterns of the tested walls at; (a) first major diagonal crack, (b) lateral peak load Q_u, and (c) when the lateral load dropped to 80% of Q_u

In general, all walls exhibited a mixed shear-flexural behaviour with a high contribution from the shear deformation towards the overall performance. Fig. 6-a shows the first major diagonal cracks for the three tested walls. It can be observed that, at axial stress of 0.0 MPa wall W-σ_n0 exhibited a weak lateral stiffness where many diagonal shear cracks can be seen compared to walls W-σ_n1.0 and W-σ_n1.5 at a higher axial stress, respectively. Also it can be noticed that by increasing the level of the axial stress, the

angle between the diagonal shear cracks and the bed joint plane, θ, increases. Furthermore, at a high level of applied lateral displacements the diagonal cracks became wider and spread along the whole area. As can be seen in Fig. 6-c, the percentage of the separated parts of the walls at failure decreases with increasing applied axial stress. This could be attributed to the enhancement of the aggregate interlocking at high level of compressive stress. Finally, the absence of the axial stress for wall W-σ_n0 increased the sliding deformation at the top course close to the failure load.

Fig. 7 shows the backbone lateral load-displacement ductility envelopes for the tested walls in addition to the contribution of the transverse reinforcement, V_s, and the combined contributions for the masonry and axial stress, $V_{(m+p)}$, in a relation with the lateral displacement ductility.

(a)

(b)

(c)
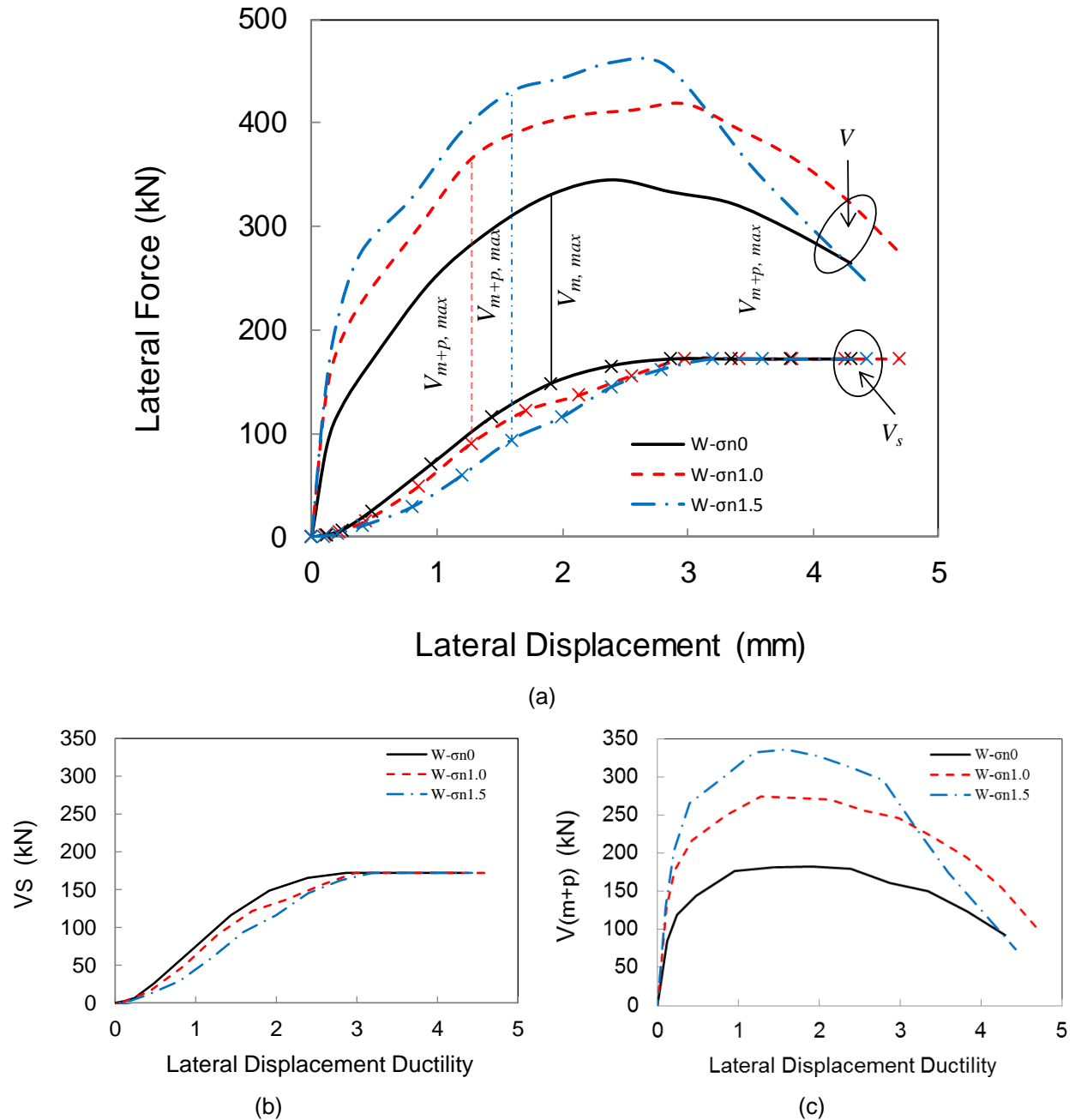
Fig. 7 – Lateral load-displacement hysteretic relationships and the backbone envelopes

The transverse reinforcement contribution, V_s, was calculated using the measured strain data along the total length of each of the transverse steel bars. The V_s for the three tested walls is presented in Fig. 7-b. Consequently, the combined contributions for the masonry and axial stress, $V_{(m+p)}$, was calculated by subtracting the transverse reinforcement contribution, V_s, from the measured lateral load (see Fig. 7-c). As shown in Fig. 7-c, The maximum combined contributions for the masonry and axial stress, $V_{(m+p)max}$, increased from 182 kN for wall W-σ_n0 to 275 and 336 kN for walls W-σ_n1.0 and W-σ_n1.5 with a contribution of the axial stress, σ_n, towards the $V_{(m+p)}$ by about 27% and 30%, respectively. However, the contribution of σ_n towards the total maximum lateral resistance V_{max} becomes about 21% and 23% for walls W-σ_n1.0 and W-σ_n1.5, respectively. As can be seen from Figure 7b, increasing the axial load delays the contribution of the transverse reinforcement, V_s. As such, increasing the axial load results in two effects; an increase in the $V_{(m+p)max}$ that is accompanied by a reduction in the corresponding V_s. Therefore, the effect of the axial stresses, σ_n, on $V_{(m+p)max}$ is higher than its effect on V_{max}.

4. Summary and Conclusions

The results of three fully grouted reinforced masonry shear walls tested under axial compressive stress of 0.0, 1.0, and 1.5 MPa respectively are presented and discussed in this paper to evaluate the influence of the axial compressive stress on the in-plane shear performance of RM shear walls.

The test results showed that the axial compressive stress, σ_n, has a considerable influence on the overall in-plane shear performance of RM shear walls. Increasing the axial compressive stress enhances the aggregate interlocking mechanism, hence delaying the initiation of the diagonal cracks. Moreover, it increases the initial lateral stiffness and shear strength of the masonry shear wall. However, for higher applied axial compression load, the tested RM shear walls exhibited higher post-peak strength degradation. In addition, delaying the initiation of the diagonal cracks for walls with higher level of axial compressive loads will lead to a delay in the contribution of the transverse reinforcement toward the RM in-plane shear force and displacement ductility capacities.

5. Acknowledgements

6. References

Anderson, D.L., and Priestley, M.J.N., "In-Plane Shear Strength of Masonry Walls", *Proceedings of the 6th Canadian Masonry Symposium*, Saskatoon, Saskatchewan, June 1992, pp. 223-234.

Banting, B., and El-Dakhakhni, W. W., "Normal strain-adjusted shear strength expression (NSSSE) for reinforced masonry structural walls", *Journal of Structural Engineering (ASCE)*, Vol. 140, No. 3, April 2013, 04013075.

CSA S304-14, "Design of Masonry Structures", *Canadian Standards Association*, 2014, Mississauga, Ontario, Canada.

El-Dakhakhni, W. W., Banting, B.R. and Miller S.C., "Seismic performance Parameters Quantification of Shear-Critical Reinforced Concrete Masonry Squat Walls," *Journal of Structural Engineering (ASCE)*, Vol. 139, No. 6, June 2013, pp. 957-973.

Matsumura, A., "Shear Strength of Reinforced Masonry Walls", *Proceedings of the 9th World Conference on Earthquake Engineering*, Vol. 7, Tokyo, Japan, August 1988, pp. 121-126.

Mayes, R.L., Omote, Y., and Clough, R. W., "Cyclic Shear Tests on Masonry Piers: Test Results", *Earthquake Engineering Research Center*, Vol. 1, Report No. Report No. *UCB/EERC-76/08*, University of California, Berkeley, May 1976. 105 pages.

MSJC-2013, "Building Code Requirements for Masonry Structures", TMS 402-13/ACI 530-13/ASCE 5-13, 2013, Masonry Standard Joint Committee.

Priestley, M. J. N., and Elder, D.McG., "Cyclic Loading Tests of Slender Concrete Masonry Shear Walls", *Bulletin NZSEE*, Vol. 15, No. 1, March 1982, pp. 3-21.

Priestley, M.J.N., Verma, R., and Xiao, Y., "Seismic Shear Strength of Reinforced Concrete Column", *Journal of Structural Engineering (ASCE)*, Vol. 120, No. 8, August 1994, pp. 2310-2329.

Seif ElDin, H.M., and Galal, K. "Survey of Design Equations for the In-Plane Shear Capacity of Reinforced Masonry Shear Walls," *Proceedings of the 12th North American Masonry Conference*, May 2015, Denver, Colorado.

Shing, P. B., Noland, J.L., Klamerus, E., and Schuller, M. (1989), "Inelastic Behaviour of Concrete Masonry Shear Walls", *Journal of Structural Engineering (ASCE)*, Vol. 115, No. 9, September 1989, pp. 2204-2225.

Shing, P.B., Schuller, M., Hoskere, V.S., and Carter, E., "Flexural and Shear Response of Reinforced Masonry Walls", *Structural Journal (ACI)*, Vol. 87, No. 6, November 1990, pp. 646-656.

Sveinsson, B.I., McNiven, H.D., and Sucuoglu, H., "Cyclic Load Tests of Masonry Single Piers", *Earthquake Engineering Research Center*, Vol. 4, Report No. UCB/EERC-85/15, University of California, Berkeley, December 1985. 188 pages.

Voon, K.C., and Ingham, J.M., "Design Expression for the In-Plane Shear Strength of Reinforced Concrete Masonry", *Journal of Structural Engineering (ASCE)*, Vol. 133, No. 5, May 2007, pp. 706-713.